Available online at www.sciencedirect.com
SCIENCE DIRECT
Agricultural water management
ELSEVIER
Agricultural Water Management 74 (2005) 219–242
www.elsevier.com/locate/agwat

Two-dimensional modeling of nitrate leaching for various fertigation scenarios under micro-irrigation

A.I. Gärdenäs [a], J.W. Hopmans [b,*], B.R. Hanson [b], J. Šimůnek [c]

[a] *Swedish University of Agricultural Sciences, Department of Soil Sciences, 75007 Uppsala, Sweden*
[b] *Department of Land, Air and Water Resources, University of California, 123 Veihmeyer Hall, Davis, CA 95616, USA*
[c] *University of California, Department of Environmental Sciences, Riverside, CA 92521, USA*

Accepted 25 November 2004

Abstract

The regular application of nitrogen fertilizers by irrigation is likely responsible for the increase in nitrate concentrations of groundwater in areas dominated by irrigated agriculture. Consequently, sustainable agricultural systems must include environmentally sound irrigation practices. To reduce the harmful effects of irrigated agriculture on the environment, the evaluation of alternative irrigation water management practices is essential. Micro-irrigation offers a large degree of control, enabling accurate application according to crop water requirements, thereby minimize leaching. Furthermore, fertigation allows the controlled placement of nutrients near the plant roots, reducing fertilizer losses through leaching into the groundwater. The presented two-dimensional modeling approach provides information to improve fertigation practices. The specific objective of this project was to assess the effect of fertigation strategy and soil type on nitrate leaching potential for four different micro-irrigation systems. We found that seasonal leaching was the highest for coarse-textured soils, and conclude that fertigation at the beginning of the irrigation cycle tends to increase seasonal nitrate leaching. In contrast, fertigation events at the end of the irrigation cycle reduced the potential for nitrate leaching. For all surface-applied irrigation systems on finer-textured soils, lateral spreading of water and nitrates was enhanced by surface water ponding, causing the water to spread across the surface with subsequent infiltration downwards and horizontal spreading of soil nitrate near the soil surface. Leaching potential increased as the difference between the extent of the wetted soil volume and rooting zone increased.

Keywords: Nitrate leaching; Fertigation scenarios; Micro-irrigation; Numerical modeling

* Corresponding author. Tel.: +1 530 752 3060; fax: +1 530 752 5262.
E-mail address: jwhopmans@ucdavis.edu (J.W. Hopmans).

0378-3774/$ – see front matter
doi:10.1016/j.agwat.2004.11.011

1. Introduction

The quality of soils, ground and surface waters is specifically vulnerable in climatic regions where agricultural production is possible only by irrigation such as in California (USA) and in many other (semi-) arid regions of the world. The regular excessive application of nitrogen fertilizers with irrigation water is likely responsible for the increase in nitrate concentrations of groundwater resources in these areas. Specifically, non-point source pollution of nitrate in groundwater is a major problem in many areas of California such as the Salinas Valley, Santa Maria Valley, and along the eastside of the San Joaquin Valley. As a result, nitrate concentrations in groundwater exceeds the drinking water standard in these areas. Therefore, alternative irrigation water and soil management practices are needed that tactically allocate water and fertilizers to maximize their application efficiency, by minimizing fertilizer losses through leaching towards the groundwater (Bar-Yosef, 1999).

The shape of the wetted soil volume under micro-irrigation and the spatial distribution of soil water, matric potentials, and nitrate concentrations are dependent on many factors, including soil hydraulic properties, emitter discharge rates, spacing, and their placement (above or below the soil surface), irrigation quantity and frequency, crop water uptake rates and root distribution patterns. Water and nutrients should not be applied in areas where roots are absent, or at a rate higher than the roots can possibly take up. In general, root development under drip irrigation is constrained to the soil volume wetted by the emitters, with root length density decreasing with depth (Goldberg et al., 1971; Stevens and Douglas, 1994; Michelakis et al., 1993). A better understanding of the interactions of irrigation method, soil type, crop root distribution, and uptake patterns and rates of water and nutrients will provide improved means for proper and efficient micro-irrigation water management practices (Hopmans and Bristow, 2002).

Micro-irrigation (drip emitters, drip tape, and micro-sprinklers) has the potential of precisely applying water and chemicals both in amount and in location throughout a field. Studies have shown the potential of high field-wide uniformity of applied water and chemicals to be higher when compared with other irrigation methods, provided that the micro-irrigation systems are properly designed, managed, and maintained. For example, the studies by Alsinan (1998) and Schwankl and Prichard (2001) demonstrated that field-wide uniformity of applied chemicals is partly controlled by the on and off times of injection, considering the travel time of applied water to move through the end-of-the-line. Micro-irrigation systems can be designed and operated so that water and nutrients are applied at a rate, duration and frequency, so as to maximize crop water and nutrient uptake, while minimizing leaching of nutrients and chemicals from the root zone of agricultural fields. While high field-wide uniformities are possible under micro-irrigation, the distribution of both water and nitrate about the drip line is very non-uniform. Both soil moisture content and chemical concentration will be the highest near the drip line after application, but will redistribute thereafter as controlled by soil physical properties. Because of these types of non-uniform wetting patterns, it is possible that percolation below the root zone and nitrate leaching occurs, despite that applied irrigation water is equal or less than crop ET. It is therefore essential to use a two-dimensional modeling

approach to develop optimal fertigation practices. The leaching potential can be changed by the timing of the fertigation, relative to the irrigation water application. A specific example of this was presented by Cote et al. (2003), demonstrating that fertigation at the beginning of the irrigation cycle might reduce nitrate leaching under specific conditions.

There are few soil and crop specific guidelines for designing and managing irrigation/fertigation systems that minimize nitrate leaching, considering typical non-uniform distributions of soil solution nitrate and crop uptake. Some studies have investigated the distribution of fertilizer about the dripline (e.g. Clothier and Sauer, 1988; Mmoloawa and Or, 2000), but few studies have investigated the effect of fertigation management/irrigation management on the spatial distribution and crop availability of supplied nitrogen (e.g. Somma et al., 1998; Mailhol et al., 2001; Li et al., 2004). Currently, the grower's incentive for adopting improved fertigation practices may be limited, since fertilizer costs are only a small fraction of the total production costs and changes in proposed fertigation practices may not affect crop yield. However, when energy costs and groundwater contamination regulations are incorporated, improved fertigation practices may be essential.

The presented study will assist operators of micro-irrigation systems to better manage fertigation, as well as their design, especially, to minimize nitrate leaching. The specific objective of this study was to evaluate the controls of fertigation strategy and soil type on nitrate leaching potential for four different micro-irrigation systems, each associated with a typical crop. The selected combinations of micro-irrigation system and crop are representative for California conditions.

2. Materials and methods

The modeling of water flow and fertigation scenarios was conducted using an adapted version of the computer simulation model, Hydrus-2D (Šimůnek et al., 1999). This software package can simulate the transient two-dimensional or axi-symmetrical three-dimensional movement of water and nutrients in soils. In presented applications, we solely considered nitrate as applied by the micro-irrigation systems through fertigation. In addition, the model allowed for specification of root water and nitrate uptake, affecting the spatial distribution of water and nitrate availability between irrigation cycles. The soil hydraulic properties parameters for the various soil types that are required for the simulation model were available in the model's database. For each soil type and emitter type, the spatial patterns of water content and nitrate concentration were determined for various fertigation strategies. These strategies included different injection durations, different injection times relative to the irrigation set time, and different concentrations. Model simulations will be presented for four different pressurized irrigation systems; each associated with a typical crop. These are surface drip tape (SURTAPE; strawberry), subsurface drip tape (SUBTAPE; processing tomatoes), surface drip emitter (DRIP; grape), and micro-sprinkler (SPR; citrus). These types were chosen as they represent a typical variety of commonly used micro-irrigation systems in California.

2.1. Micro-irrigation modeling

Considering two-dimensional soil water flow, the water flow equation is written as:

$$\frac{\partial \theta}{\partial t} = \frac{\partial}{\partial r}\left(K_r \frac{\partial h}{\mathrm{d}r}\right) + \frac{\partial}{\partial z}\left(K_z \frac{\partial h}{\partial z}\right) - \frac{\partial K}{\partial z} - \mathrm{WU}(h, r, z) \quad (1)$$

where θ is the volumetric soil water content (L^3L^{-3}), K defines the unsaturated hydraulic conductivity function (LT^{-1}), h is the soil water pressure head (L), r is the lateral coordinate, z is the vertical coordinate (positive downwards), t is time (T) and WU(h, r, z) denotes root water uptake (T^{-1}). Both K and WU are functions of θ and/or h. The subscripts r and z allows for the possibility to include soil anisotropy, i.e. to simulate water flow with the unsaturated hydraulic conductivity function being different for the r- and z-direction. Two-dimensional flow was used for both the surface and subsurface drip tape (SURTAPE and SUBTAPE) systems. The axi-symmetrical form of Eq. (1) was used to solve for the radial flow equation to simulate water and nutrient distribution for both the surface drip emitter (DRIP) and micro-sprinkler (SPR) system. For simplicity of notation, we use the same spatial coordinate notation, r, for both radial and horizontal directions. In both cases, Eq. (1) was solved with the Hydrus-2D model (Šimůnek et al., 1999) using the Galerkin finite element method based on the mass conservative iterative scheme proposed by Celia et al. (1990). We used the hydraulic relationships as defined by van Genuchten (1980).

For all simulated scenarios, it was assumed that lateral water flow along the boundaries was zero (zero flux boundary condition), and that the bottom boundary is defined by a unit vertical hydraulic gradient, simulating free drainage from a relatively deep soil profile. The top boundary condition representing irrigation events vary according to the simulated irrigation system. However, for all scenarios, the crop-specific potential evapotranspirative flux (ET_c) was computed from the product of potential evapotranspiration (ET_0) and the crop coefficient (K_c). In all scenarios, except for DRIP, it was assumed that the potential evapotranspiration was equal to the potential crop transpiration, T_{pot}, thus neglecting evaporation. For the DRIP scenario, the potential ET was partitioned into potential evaporation ($E_p = 0.05ET_c$) and potential transpiration ($T_p = 0.95ET_c$).

During irrigation, the particular boundary conditions representing various irrigation systems were of the flux type, controlled by the constant volumetric application rate (Q_0, L^3T^{-1}) of the emitter of each micro-irrigation system. The Hydrus-2D code was adapted to allow for a time-variable ponded boundary condition by computing wetted surface area. This was done by switching from a Neumann (flux) to a Dirichlet (head) boundary condition if the surface pressure head required to accommodate the specified emitter flux for a surface node, is larger than 0. A sufficient number of surface nodes are switched in an iterative way until the entire irrigation flux Q_0 is accounted for, and the radius of the wetted area is obtained. Since the infiltration flux into the dry soil is larger for early times, the wetted area continuously increases as irrigation proceeds.

Numerical solutions were confirmed through comparison of the wetted radius with the steady state analytical solution of Wooding (1968). In addition, the Hydrus-2D code was adapted to compute positive soil water backpressure values for the SUBTAPE system

(Lazarovitch et al., 2005) that develop if the flow rate out of the drip tape is larger than the rate at which the discharged water can move into the wetted soil surrounding the drip tape.

The local root water uptake term in Eq. (1) was computed from:

$$\mathrm{WU}(h,r,z) = \gamma(h)\mathrm{RDF}(r,z)WT_{\mathrm{pot}} \tag{2}$$

where $\gamma(h)$ is the so-called soil water stress response function (dimensionless) of Feddes et al. (1978) that reduces root water uptake from its maximum possible value because of soil water stress. RDF denotes the normalized root water uptake distribution, T_{pot} is the potential transpiration rate, and W is the width or radius of the soil surface, associated with the transpiration process (as controlled by the lateral root distribution). Both $\gamma(h)$ and RDF are a function of the spatial position within the multi-dimensional root zone domain. The RDF function was normalized, so that when integrated over the root zone (Ω) domain, its value is equal to 1, i.e.

$$\mathrm{RDF}(r,z) = \frac{\beta(r,z)}{\int_{\Omega}\beta(r,z)\mathrm{d}\Omega} \tag{3}$$

where β characterizes the dimensionless spatial distribution of unstressed root water uptake. For the non-uniform cases, RDF was defined by (Vrugt et al., 2001):

$$\beta(r,z) = \left[\left(1-\frac{z}{z_{\mathrm{m}}}\right)\right]\left[\left(1-\frac{r}{r_{\mathrm{m}}}\right)\right]\mathrm{e}^{-((p_z/z_{\mathrm{m}})|z^*-z|+(p_r/r_{\mathrm{m}})|r^*-r|)} \tag{4}$$

where r_{m} and z_{m} define the maximum rooting length in the radial/horizontal direction and depth direction (L), and p_z, z^*, p_r, and r^* are empirical parameters that can describe non-symmetrical root geometries. The physical interpretation of these parameters is presented in Vrugt et al. (2001). For the uniform root distribution cases, RDF = $1/Wz_{\mathrm{m}}$. In the presented simulations, we assumed that the root distribution is constant in time.

In Hydrus-2D (Šimůnek et al., 1999), solute transport is described by

$$\frac{\partial\theta c}{\partial t} = \frac{\partial}{\partial x_i}\left(\theta D_{ij}\frac{\partial c}{\partial x_i}\right) - \frac{\partial q_i c}{\partial x_i} - \mathrm{NU}(c,r,z,t) \tag{5}$$

where the subscripts i and j denote either r or z, and c denotes the nitrate concentration in soil solution (ML^{-3}). The first term on the right side represents the solute flux due to dispersion, the second term the solute flux due to convection with flowing water, and the third term represents root nutrient uptake. The water flux q is computed from Eq. (1), D_{ij} is the dispersion coefficient ($\mathrm{L}^2\mathrm{T}^{-1}$), and the NU term defines the local passive nitrate uptake ($\mathrm{ML}^{-3}\mathrm{T}^{-1}$) by plant roots, which is a function of time and the spatial coordinates. The presented application assumes a single value for the longitudinal dispersivity of 5 cm (with the transverse dispersivity being one-tenth of the longitudinal dispersivity), and neglects molecular diffusion. For all applications, the initial relative nitrate concentration is 0. The boundary condition representing fertigation is a third-type Cauchy boundary condition that prescribes the fertigation rate during defined irrigation intervals. The solute flux is defined by the product of the spatially variable water infiltration rate, q_0 (LT^{-1}), and the dissolved nitrate concentration, c_0 (ML^{-3}). We assume no lateral transport of nitrate outside the domain boundaries. The cumulative leaching of nitrate mass out of the lower boundary is controlled by the nitrate concentration at that depth and the corresponding water flux

density as computed from Eq. (1). At all times, the spatially distributed nutrient-uptake term, NU, is computed from

$$\mathrm{NU}(r,z,t) = c(r,z,t)\mathrm{WU}(r,z,t) \tag{6}$$

using the local WU value as computed from solution of Eq. (2). In our simulations, we limit ourselves to nitrate-N only, and neglect mineralization gains and denitrification losses.

2.2. Irrigation scenarios

A total of 80 fertigation scenarios for four different micro-irrigation systems, four different soil types, and five fertigation strategies were examined to evaluate water and nutrient use efficiency and nitrate leaching. Each of the fertigation scenarios was preceded by 56 days of flow-only simulations, to approach a 'pseudo-equilibrium' condition before irrigation with fertigation started. This was done to ensure that the initial soil water regime was not a factor in the transport and leaching predictions. The initial condition for this initialization period was set to a uniform soil water pressure head of −400 cm. The subsequent simulation period with fertigation was 28 days. The four micro-irrigation/cropping systems were (SPR) micro-sprinkler for citrus; (DRIP) drip emitter on the soil surface for grape; (SURTAPE) surface drip tape for strawberry; and (SUBTAPE) subsurface drip tape for processing tomatoes. All micro-irrigation systems were applied to four different soil types: sandy loam (SL), loam (L), silty clay (C) and anisotropic silty clay (AC). The soil hydraulic parameters for the loam and sandy loam were taken from Carsel and Parish (1988) and for the silty clay from the Rosetta database (Schaap and Leij, 1998). The difference between the C and AC soil is that the lateral hydraulic conductivity of the AC soil was five times higher than for the C soil. This was accomplished by increasing the horizontal K_s of the AC soil with a factor of 5. The l-value of the VGM expression was set equal to 0.5 for all soils. Whereas the hydraulic parameter values are listed in Table 1, the corresponding functions are presented in Fig. 1.

The five simulated fertigation strategies were based on recommendations of the micro-irrigation industry and grower's practices. Schematically, the five different fertigation strategies are presented in Fig. 2. These are (B) fertigation for a total duration of 2 h, starting 1 h after the beginning of the irrigation cycle; (M) fertigation for a total duration of 2 h, in the middle of an irrigation cycle; (E) fertigation for a duration of 2 h, starting 3 h before irrigation cutoff; (M50) alternating irrigation, starting the first and last 25% of each irrigation with fresh water, and fertigation during the remaining 50% in the middle of the irrigation cycle; and (C) continuous fertigation, with 1-h fresh water irrigation before and

Table 1
Soil hydraulic properties for the four selected soil types

Textural class	θ_r ($\mathrm{cm^3\ cm^{-3}}$)	θ_s ($\mathrm{cm^3\ cm^{-3}}$)	α ($\mathrm{cm^{-1}}$)	n	K_s (cm/day)
Sandy loam, SL	0.065	0.41	0.075	1.89	106.1
Loam, L	0.078	0.43	0.036	1.56	24.96
Silty clay, C	0.111	0.481	0.0162	1.32	9.61
Anisotropic clay, AC	0.111	0.481	0.0162	1.32	$K_{s,z} = 9.61$, $K_{s,r} = 48.1$

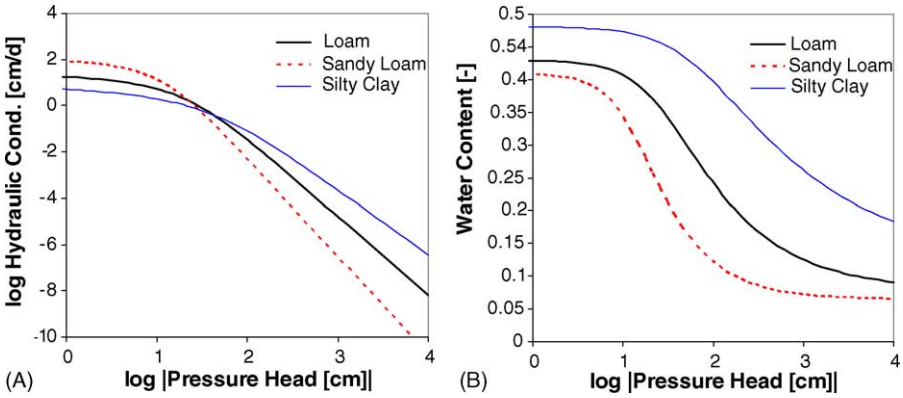

Fig. 1. Soil hydraulic relationships between (A) log hydraulic conductivity and log soil water pressure head and (B) water content and log soil water pressure head.

after the fertigation period. The fresh water irrigations prior and after each fertigation are common practices that ensure uniformity of fertilizer application and flushing of the drip lines. Fresh water time intervals were reduced to 25% for the SURTAPE irrigation because of its small irrigation interval (see Table 2). Each irrigation cycle was simulated for 28 days, including either four (SPR) or eight (DRIP, SUBTAPE and SURTAPE) irrigation cycles with fertigation. The irrigation cycle length (P) and other crop-specific irrigation characteristics are presented in Table 2. To illustrate long-term implications, the fertigation strategies were simulated for an additional 28 days for the SUBTAPE irrigation system.

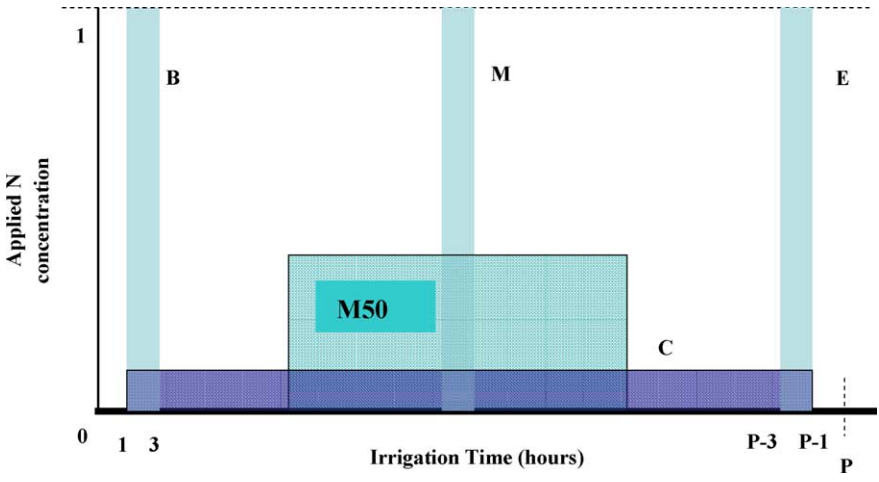

Fig. 2. A general schematic, illustrating the five fertigation strategies, where P denotes the irrigation cycle period (h). Applied concentration levels were selected such that the total applied mass was identical between scenarios. The duration of strategies B, M and E is 2 h.

Table 2
Irrigation system parameters

	SPR (citrus)	DRIP (grape)	SURTAPE (strawberry)	SUBTAPE (tomatoes)
Irrigation				
Discharge rate, Q_0 (L/day)	907.2	90.72	15.967	11.975
Irrigation intensity, q_0 (cm/day)	2.03	1.63	10.64	2.66
Irrigation time, P (day)	1.8	1.5	0.13	1.15
Irrigation interval, ΔP (day)	7	3.5	3.5	3.5
Emitter (d) and line (w) spacing (cm)	669 × 669	183 × 304	20 × 76.2	30 × 150
Depth of emitter (cm)	0	0	0	20
Water demand				
ET_0 (cm/day)	0.7	0.7	0.5	0.7
Crop coefficient, K_c	0.65	0.85	0.7	1.06
Simulated domain				
Width, W (cm)	n.a.	n.a.	75	75
Radius, R (cm)	334.5	90	n.a.	n.a.
Depth, Z (cm)	200	200	61	100
Root water uptake				
The critical water pressure heads in Feddes et al. (1978) model h_1, h_2, h_{3max}, h_{3min}, h_4 (cm)	−10, −25, −400, −400, −8000	−1, −2, −1000, −1000, −8000	−10, −25, −200, −300, −8000	−1, −2, 800, −1500, −8000
Root zone				
Root distribution model	Uniform	Vrugt model	Uniform	Vrugt model
Maximum rooting depth, z_m (cm)	100	90	30.5	100
Depth with max root density, z^* (cm)	n.a.	0	n.a	25
Maximum lateral root extension, r_m (cm)	334.0	25	56	75
Distance r with max root density, r^* (cm)	n.a.	0	n.a	0
Non-symmetry coefficients, p_z and p_r	n.a.	1.0, 1.0	n.a	1.0, 1.0

n.a. = not applicable.

2.3. Irrigation system parameters

The irrigation requirement, Q_{req} (L/day), was computed from the crop-specific potential ET_c (cm/day) and the irrigated soil area, $A = dw$, where d (cm) and w (cm) represent emitter distance and irrigation line distance, respectively. Selected ET_0 values were typical values for CA irrigated systems in the regions. The applied irrigation volume per irrigation cycle, I [cm^3], was estimated for each crop from Q_{req}, the irrigation interval, ΔP [day], and the irrigation efficiency, f_i. For all irrigation systems, we assumed an irrigation efficiency of 85%. Finally, the irrigation cycle duration, P (per day), was determined from the total irrigation volume, I, and the emitter discharge rate, Q_0. Specific values for each of the four micro-irrigation systems are presented in Table 2.

The irrigation layouts for each of the four micro-irrigation systems with characteristic dimensions, including emitter and irrigation line spacing, are presented in Fig. 3, whereas relevant irrigation application and model parameters are presented in Table 2. Both DRIP (Fig. 3A) and SPR (Fig. 3D) are considered point sources so that radial geometry is assumed. Because of the multiple outlets along the tape, both SUBTAPE (Fig. 3B) and SURTAPE (Fig. 3C) were simulated using the line-source model with a rectangular geometry. For SPR, we assumed a measured non-uniform water application with most of the applied water occurring within a 1 m radius from the sprinkler head. More detailed information about the simulation model and model parameters can be found in Hanson et al. (2004), which is available upon request.

The selected parameters for Feddes et al. (1978) water stress response function were taken from Van Dam et al. (1997), and are presented in Table 2. The values of the root distribution parameters in Table 2 signify typical root systems for the four irrigated cropping systems.

3. Results and discussion

The relative root distribution and temporal dynamics of water content and solute concentration for the four micro-irrigation systems are shown in Fig. 4A (DRIP and SUBTAPE) and b (SURTAPE and SPR), for a variable number of observation points during the 28-day irrigation period. In the interest of saving space, we only show these simulation results for the loamy (L) soil and the beginning (B) fertigation scenario. The dynamics of irrigation and fertigation is clearly demonstrated by the number of peaks. It appears that water content values have approached a quasi steady state for almost all observation points, with the exception of the observation nodes at the bottom of 2-m deep profiles (DRIP and SPR). Concentration values show that most dynamics occurs near the emitter or at the soil surface, with concentrations increasing during the 28-day period for most other regions of the soil zone.

The water balance results for all four micro-irrigation systems and soil types is summarized in Fig. 5, expressed in percent of total applied water for the 28-day period after 2 months initialization. The root zone storage was computed from the simulated root zone, whereas drainage values include water storage values below root zone in addition to the simulated water flux values at the bottom of the simulated soil domain. We conclude that

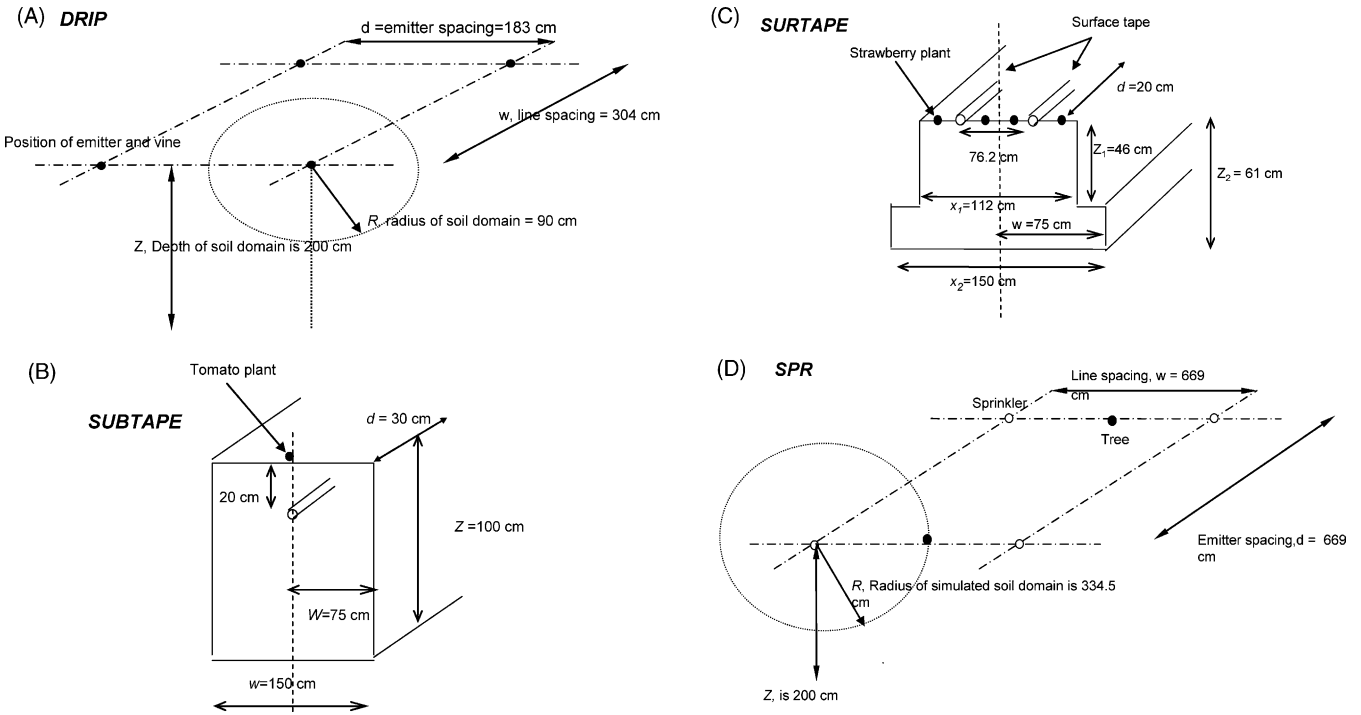

Fig. 3. Irrigation layout of the four simulated micro-irrigation systems; (A) DRIP, (B) SUBTAPE, (C) SURTAPE, and (D) SPR.

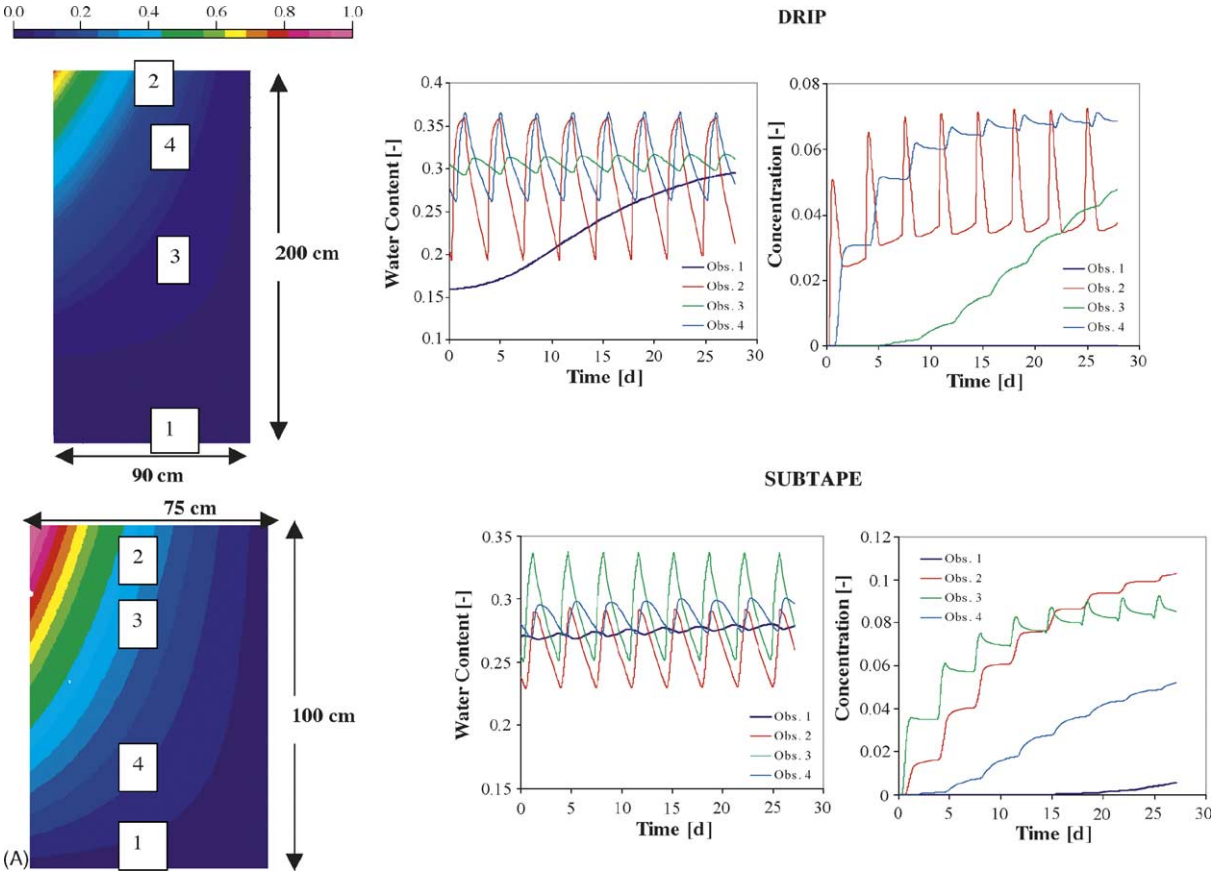

Fig. 4. Relative root distribution with location of observation nodes (left) and temporal variations in water content (middle) and nitrate concentration (right) for (A) DRIP (four observation points) and SUBTAPE (four observation points) and (B) SURTAPE (three observation points) and SPR (six observation points).

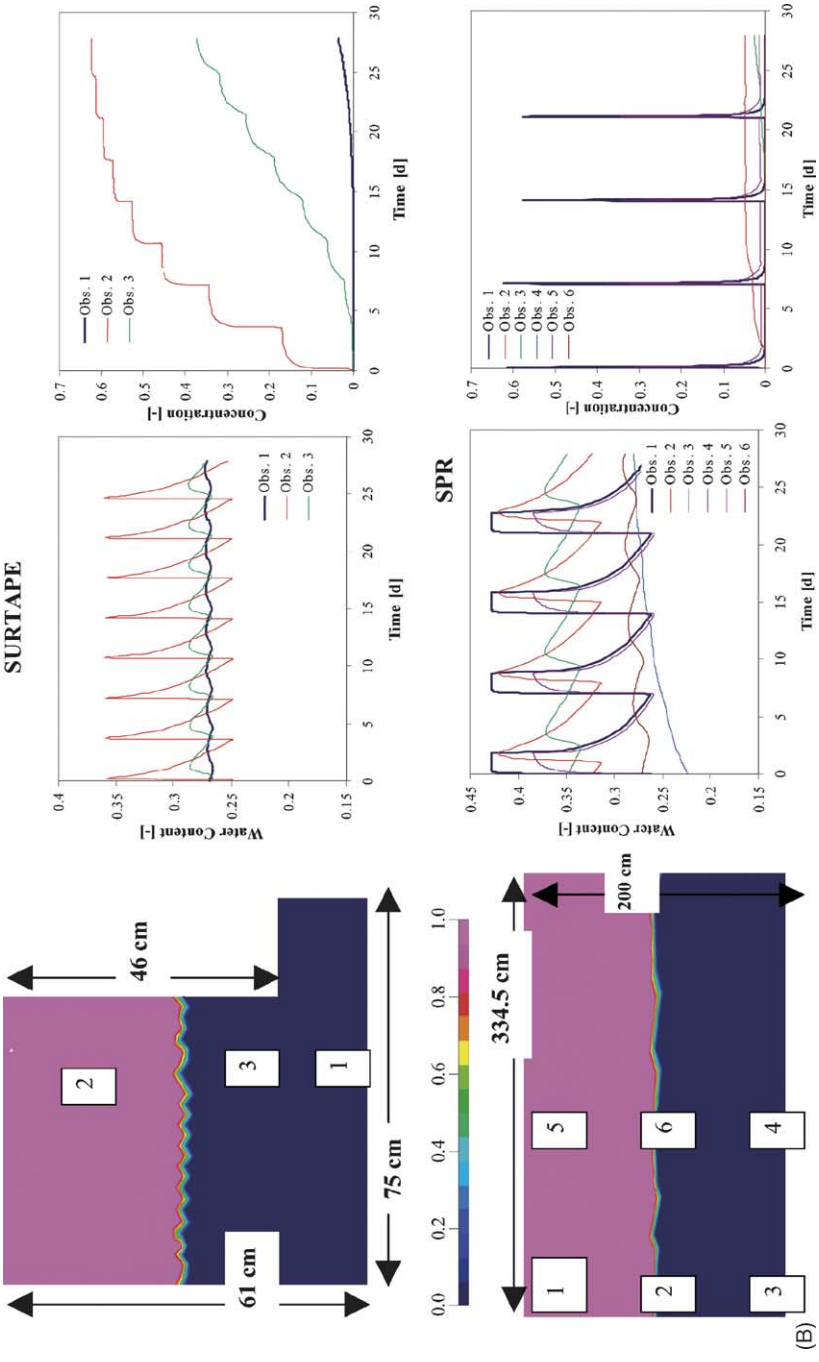

Fig. 4. (*Continued*).

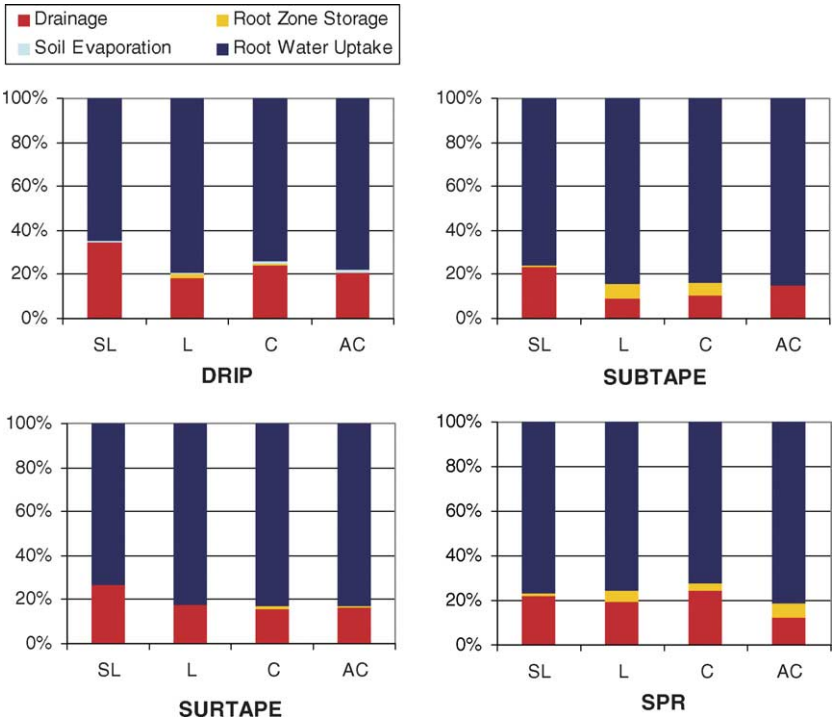

Fig. 5. Water balance for all four irrigation systems.

most of the applied irrigation water is indeed beneficially used through root water uptake, with a value of about 80%. As expected, most drainage occurs in general for the coarser-textured soils. The slightly larger drainage values for the DRIP system are likely caused by the high root density close to the soil surface and emitter, with relative low root density below the 40 cm depth. In contrast the lowest drainage values were determined for the SUBTAPE system. Over the 28-day period, soil water storage increased slightly for the SPR and SUBTAPE systems, most likely because these two systems had not reached pseudo equilibrium after the 2-month initialization period. The flow simulations assumed a well-maintained irrigation system, so that the simulated leaching data approximately agree with the irrigation requirements that were based on an irrigation efficiency, f, of 85%.

The overall N-leaching results are presented in table format in Table 3. The effective N-leaching was computed from the mass leaving the bottom of the simulated soil domain during the 1-month simulation period, augmented with the change in N-storage in the soil domain below the root zone, effectively quantifying the mass of nitrate moving out of the root zone. Thus, it was assumed that the soil N below the root zone would not be available for root uptake after the simulation period. We note that the total N-added is the same for each fertigation strategy, but varies between micro-irrigation systems. However, irrespective of irrigation system, we assume a relative nitrate concentration of 1.0 for the 2-h fertigation scenarios. Average values of percentage N leached are system-specific for each soil type, whereas the standard deviation values (S.D.) are an indication of the

Table 3
Percentage of N leached as a fraction of the total N added

Soil type	Fertigation strategy	% N leached of total N added			
		SPR	DRIP	SURTAPE	SUBTAPE
SL	B	12.976	22.571	23.115	6.647985
	M	10.295	33.1525	23.120	8.650231
	E	7.601	13.4192	22.680	6.589420
	M50	10.336	28.5178	22.685	7.898884
	C	10.319	32.0471	23.322	8.432919
	Average	10.30	25.94	22.98	7.64
	S.D. (CV, %)	1.90 (18)	8.13 (31)	0.29 (1.3)	0.98 (13)
L	B	7.642	9.1958	13.020	0.191043
	M	5.867	7.2011	12.275	0.194873
	E	4.221	2.7820	11.368	0.138668
	M50	5.893	6.6879	12.131	0.184335
	C	5.884	6.9989	12.379	0.192725
	Average	5.901	6.573	12.235	0.180
	S.D. (CV, %)	1.21 (20)	2.33 (35)	0.59 (5)	0.024 (13)
C	B	1.641	1.9637	3.596	0.015284
	M	0.896	*0.4542*	8.140	0.015739
	E	0.431	0.7813	13.849	0.007894
	M50	0.951	*0.9107*	10.449	0.014177
	C	0.912	0.8215	6.582	0.015451
	Average	0.966	0.986	8.523	0.014
	S.D. (CV, %)	0.43 (43)	0.57 (58)	3.88 (46)	0.003 (21)
AC	B	0.204	0.0366	4.302	0.000013
	M	0.100	0.0153	8.649	0.000008
	E	0.042	0.0072	14.232	0.000003
	M50	0.109	0.0194	10.626	0.000008
	C	0.103	0.0159	7.615	0.000008
	Average	0.112	0.019	9.085	0.000
	S.D. (CV, %)	0.059 (55)	0.011 (57)	3.677 (40)	0.00 (0)

variation between fertigation strategies for each system. The smaller the CV (%) value, the less impact fertigation strategy will have on controlling leaching potential. We note though that the CV values have not much meaning for average leaching fraction values lower than 1%.

3.1. Soil type effects

The results in Table 3 clearly show that soil type effects are much more important than fertigation strategy or micro-irrigation system type. Across the board, the leaching potential is much larger for the coarser-textured soils (types SL and L). Except for the SURTAPE, leaching losses are small for the C and AC soil types, independent of fertigation strategy. Also, we found that the SURTAPE irrigation scenario has the largest leaching potential, independent of soil type or fertigation strategy. First, the root zone is shallow, confined to the 30 cm depth. Hence, applied irrigation water will be lost if redistributed

water moves below this depth. This is likely the main cause for the coarse-textured soils. Secondly, for the finer-textured soil types, the infiltration capacity is limited, causing a significant fraction of the applied water to move laterally across the soil surface into the furrows. This water moves subsequently back into the soil; however, it is essentially lost because the furrow depth is below the assumed maximum rooting depth (see also Fig. 9). The lowest overall leaching losses for the AC soil are the result of lateral movement of water and dissolved fertilizer, thereby making more effective use of the whole rooting system.

3.2. Irrigation system effects

In general, the leaching potential increases from SUBTAPE, SPR, DRIP to SURTAPE. An exception to this general result is large leaching value for the DRIP system for the SL soil, caused by the high hydraulic conductivity and low soil water storage capacity of the coarse-textured soil in combination with limited lateral spreading of roots.

3.3. Fertigation strategy effects

In general, we found that the largest leaching losses occur most often for the B fertigation strategy (in 9 out of 16 cases). This is so because its fertigation period is the smallest (as are M and E) and nitrate is potentially available for leaching during the subsequent irrigation period. A potential exception applies for the SUBTAPE irrigation system, for which the leaching potential was reduced for the B-fertigation strategy, once the fertigation period was extended from 28 to 56 days, especially for the coarse-textured soils (results not shown). This result is in agreement with sandy soil simulations of Cote et al. (2003), who concluded that the higher retention of nutrients for the B strategy is caused by the upward transport of nutrients during and immediately after the fertigation by capillary movement. However, their general conclusion was based on irrigation in extremely dry soils, neglecting root water uptake. The E scenarios are most efficient and generate the least leaching. However, we note that of the total of 16 soil type/irrigation system combinations in Table 3, only six of those have an average leaching above 1%. Yet, fertigation strategy E generated the least leaching among the five strategies for these six worst-case scenarios.

An exception to this general rule applies to the SURTAPE irrigation system where the leaching of the E strategy is relatively high for all soil types, in particular for the finer-textured soils (C and AC). For these systems, the likelihood of surface losses by lateral flow are the highest, thereby increasing the percent N losses. In addition, because of the short irrigation times for the SURTAPE system (0.13 days in Table 2), differences between fertigation strategies, as expressed by CV in Table 3, are the lowest for SURTAPE. Except for the SURTAPE, leaching losses are small for the C and AC soil types, independent of fertigation strategy. The type of fertigation has the largest effect for the DRIP system, most likely because of its relatively small rooting zone size.

Additional variations in leaching between fertigation scenarios are likely caused by differences in spatial extent between the wetting soil volume and root domain. Leaching losses are most likely to occur for irrigation/fertigation scenarios where the differences in

wetting and root volumes are large. It is therefore that some DRIP systems are most vulnerable to leaching, and that leaching occurs for non-uniform water applications for the SPR system.

3.4. Nutrient uptake

Although not shown here, root nutrient uptake accounted for about 40–60% of the total N added, independent of fertigation scenario. Root nitrate uptake was the least for the SPR irrigation system (20–30%), mostly caused by the highly non-uniform water application, whereas roots extended laterally through the simulated soil domain. Consequently, both water and nutrients were less accessible for the roots further away from the sprinkler system. Most of the applied nitrate (50–80%) was stored in the root zone, potentially vulnerable for leaching after 28 days, later in the growing season.

3.5. Specific results

The effects of soil type and fertigation strategy using DRIP on soil nitrate distribution is presented in Fig. 6, using contour plots of relative nitrate concentration. These plots allow for a qualitative interpretation of the simulation results, regarding leaching potential. All results are representative for the end of the first irrigation cycle of duration P (Table 2). Therefore, subsequent water and nitrate distribution will be controlled by additional irrigation cycles, followed by soil water redistribution and root water and nitrate uptake. Most results are intuitively clear, with nitrate occurring at larger depths for the coarser-textured soils. Nitrate concentrations are increasingly diluted for the fertigation strategies that have longer nitrate application times (M50 and C) and longer periods of freshwater application after fertigation (B and M). Hence, typically the highest nitrate concentrations occur for the E fertigation strategy that applies the nitrate in a 2-h period at the end of the irrigation cycle. We note that the rootzone is concentrated in a 30 cm circle around the drip line (Fig. 4A). Therefore, the E-strategy is most efficient, as it applies the nitrate to the roots and minimizes leaching. Finally, the increased lateral spreading of the nitrate in the silty clay soils is mostly caused by the increased ponded soil surface, as controlled by the infiltration rate. Also, anisotropy clearly leads to enhanced lateral transport of water and dissolved nitrate, reducing nitrate leaching potential and making nutrients available near the soil surface where roots are generally most abundant.

Similar contour plots for the SUBTAPE irrigation system are presented in Fig. 7. As for DRIP, the highest nitrate concentrations occur near the emitter. Since the drip tape is buried, there is no enhanced lateral spreading of the nitrate across the wetted soil surface or for the anisotropic clay soils, as was the case for DRIP. The relative root distribution for this system has most roots available for nutrient uptake in a circle of about 40 cm around the drip tape, with a maximum root density at the 25 cm depth (Table 2).

Fig. 8 shows the concentration contour plots for the SURTAPE micro-irrigation system. Most striking about these results is that the occasional ponding of the soil surface extends beyond the bed surface for the finer-textured soils (C and AC), causing water accumulation in the furrow and allowing for infiltration of water with dissolved nitrate into the bed at the 40 cm depth. Since the rooting depth was limited to the 30 cm depth, this adds to increased

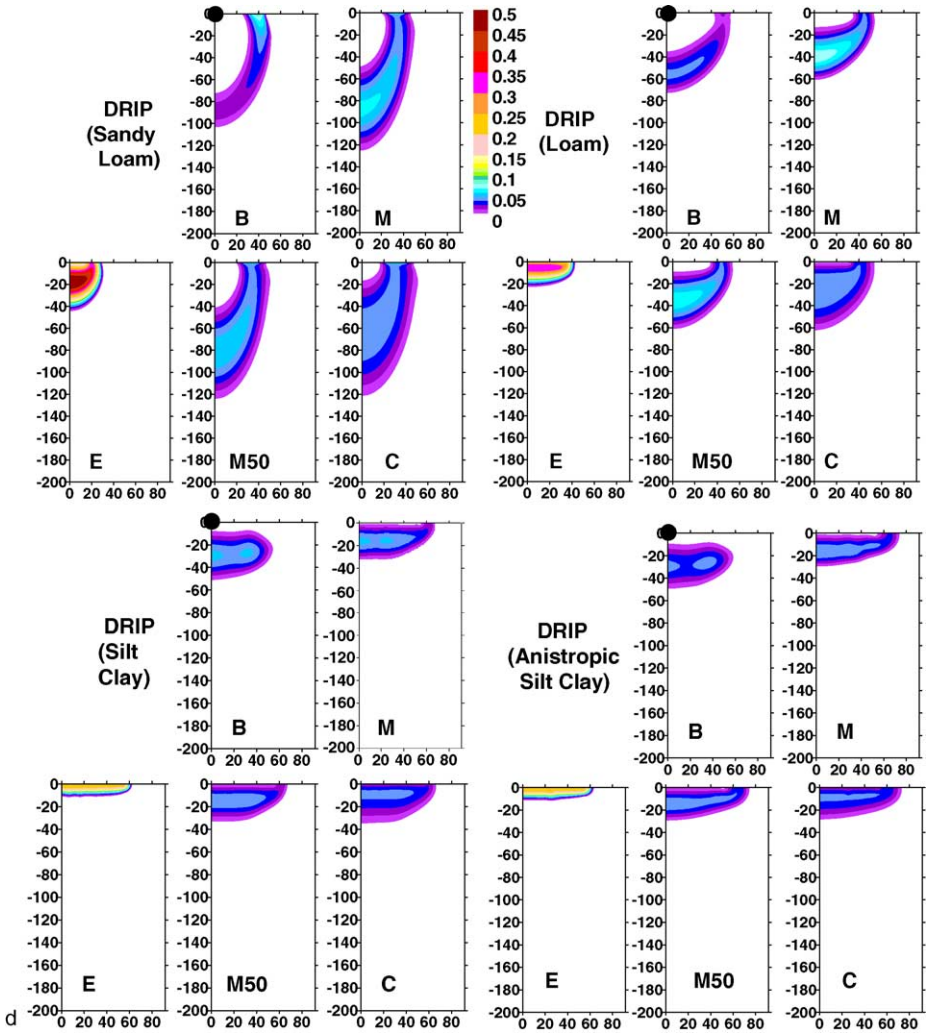

Fig. 6. Contour plots of relative nitrate concentration for DRIP, four soil types and five irrigation strategies.

water and nutrient losses. In all other aspects, the SURTAPE system performs as the other systems with the lowest leaching potential for the E fertigation strategy.

Many micro-sprinkler systems apply water non-uniformly, as the one that is used in our simulations for which the concentration contour plots are presented in Fig. 9. Because we assumed that roots were uniformly distributed in the lateral direction to a depth of 100 cm, the non-uniform application leads potentially to large leaching losses in the soil domain near the sprinkler head. However, as before, the E-fertigation strategy is likely the most efficient as it eliminates leaching by fresh water after fertigation. If roots can take up the nutrients before the front reaches the 100 cm rooting depth, leaching losses will be small. Both the C and AC (anisotropic clay) allow for increases lateral movement of the water and

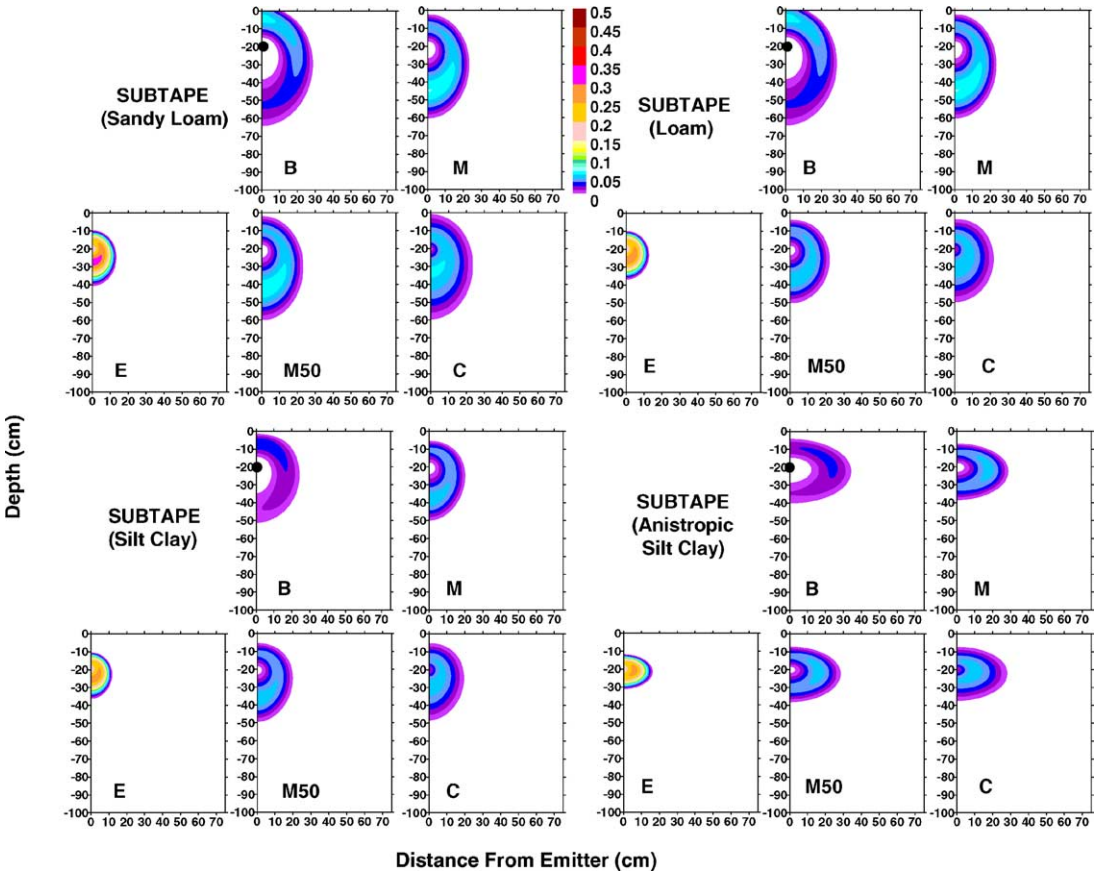

Fig. 7. Contour plots of relative nitrate concentration for SUBTAPE, four soil types and five irrigation strategies.

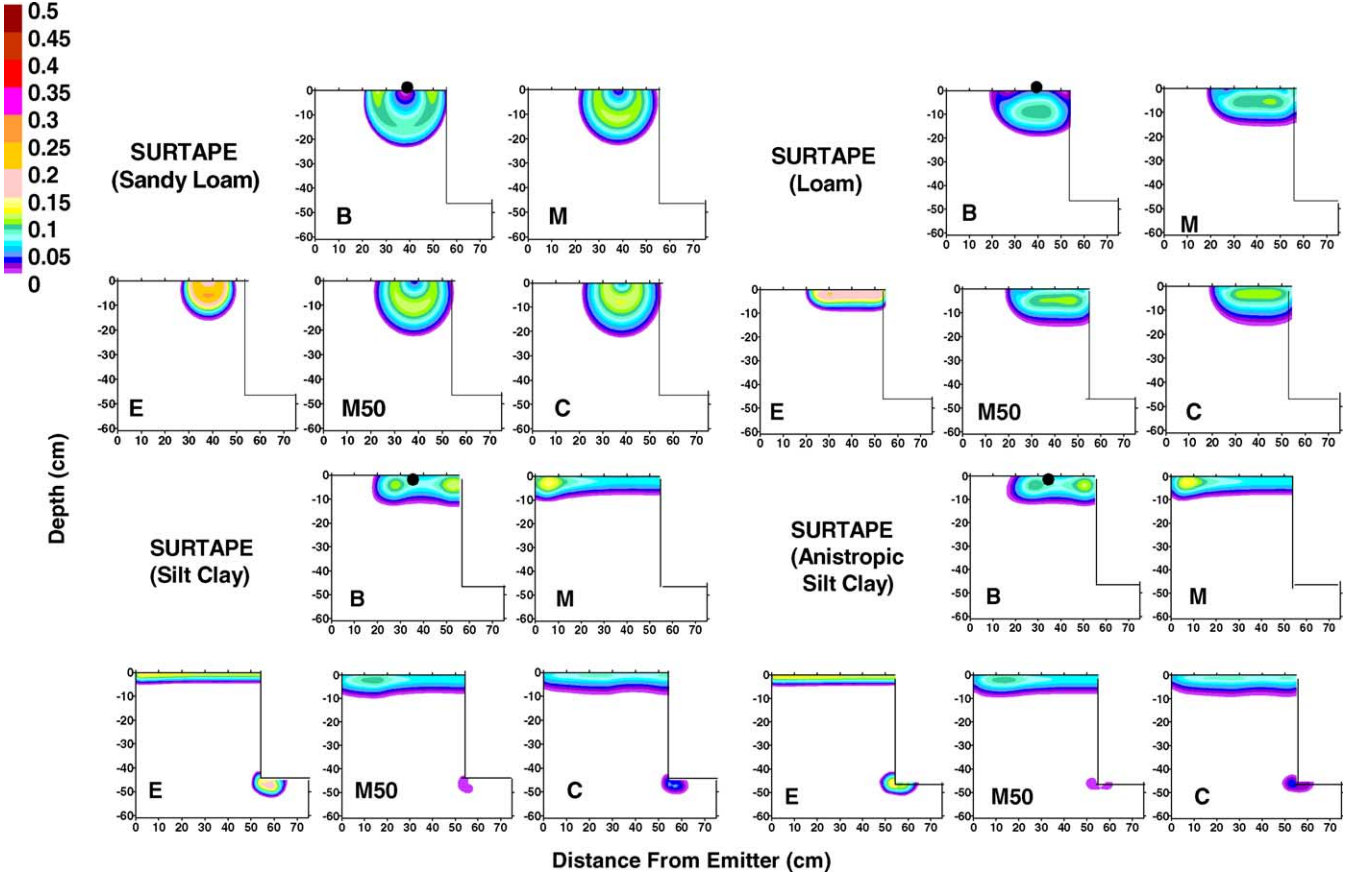

Fig. 8. Contour plots of relative nitrate concentration for SURTAPE, four soil types and five irrigation strategies.

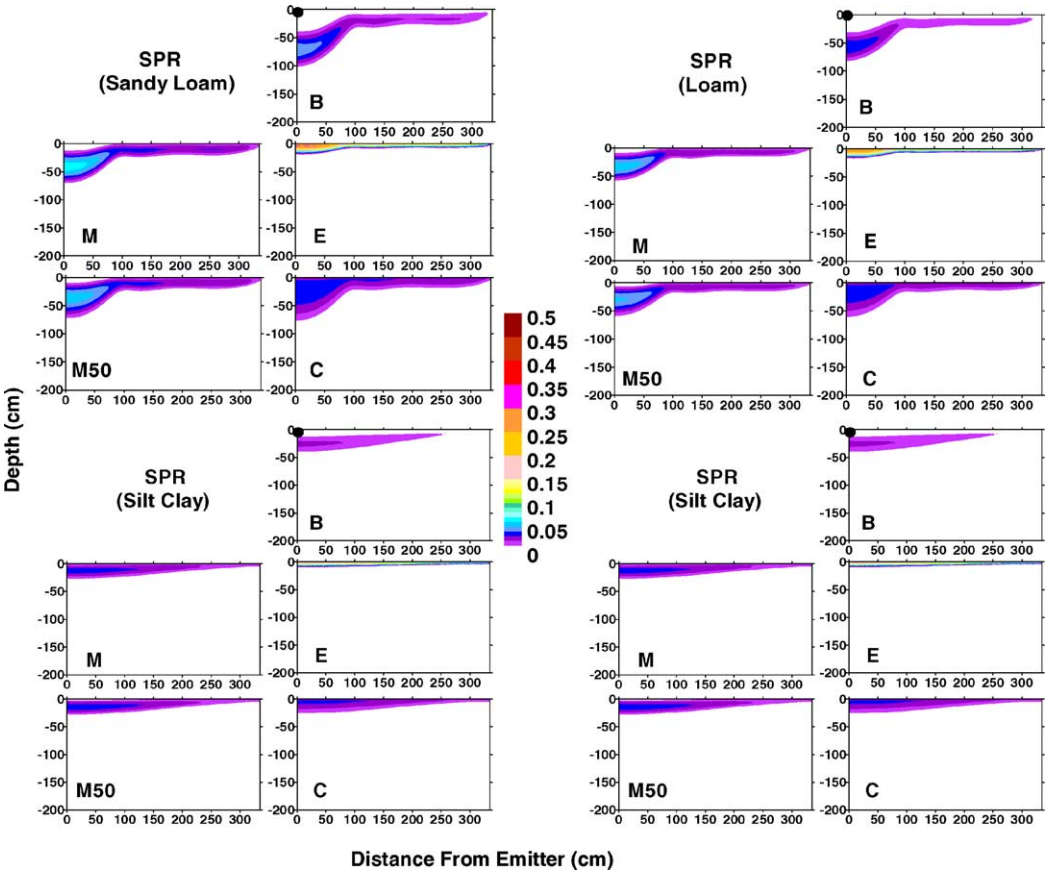

Fig. 9. Contour plots of relative nitrate concentration for SPR, four soil types and five irrigation strategies.

dissolved nitrate, thereby making nitrate more available to the roots and reducing leaching potential.

There is little information on soil nitrate distributions, both experimental and through numerical model simulations. Specifically, no field experimental data for various fertigation strategies are available. The modeling study by Cote et al. (2003) demonstrated that fertigation strategy can affect nitrate leaching. Modeling studies by Abbasi et al.

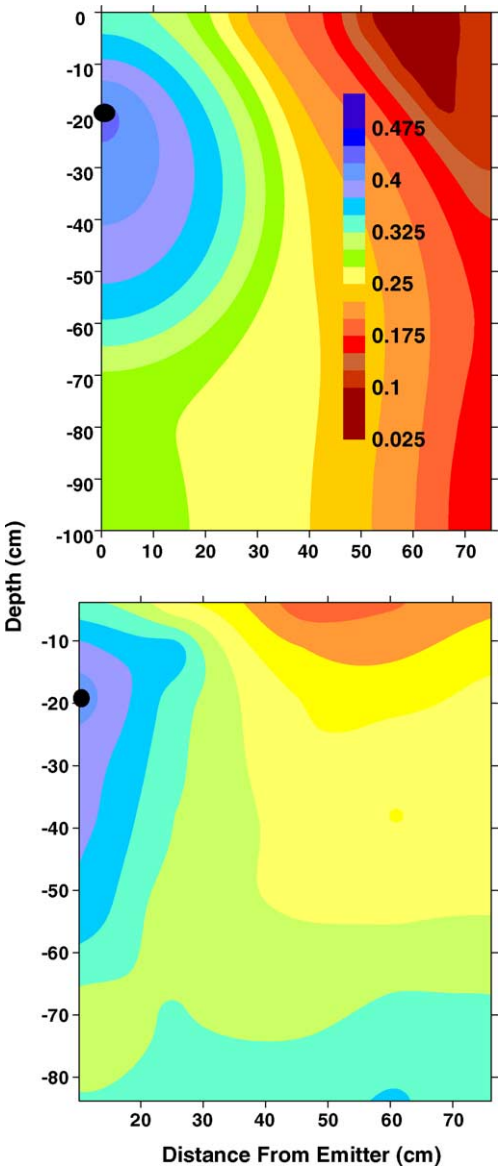

Fig. 10. Comparison of measured and simulated spatial water content distributions of SUBTAPE.

(2003a, 2003b) and Assouline (2002) showed that Hydrus-2D simulations of soil water content and solute distributions are reasonably close to measured values. As also demonstrated by the laboratory study of Li et al. (2004), field nitrate distributions are highly affected by the wetting patterns of the micro-irrigation system. A comparison of wetting patterns between field measurements (Hanson, unpublished data) and Hydrus-2D simulations for the subsurface drip irrigation of tomatoes is presented in Fig. 10. For both, soil water content values were maximal near the drip line and decreased with depth below the drip line and with horizontal distance. Soil water content increased with depth above the drip line. The experimental data showed some elongation in the vertical direction, probably reflecting preferential flow channels in the soil, which were not simulated by Hydrus-2D. Also Skaggs et al. (2004) concluded that Hydrus-2D predictions of water content distribution for drip tape irrigation agreed well with experimental observations. In addition to not including soil structural effects, we realize that the presented model results may be different if soil nitrogen chemistry is an important aspect of transport.

4. Conclusions

In summary, we report on the results of using the current state-of-the-art modeling of micro-irrigation systems, with a specific emphasis on fertigation strategies that affect nitrate leaching. When comparing micro-irrigation systems and fertigation strategies, the soil type must be considered. Seasonal leaching was the highest for the sandy loam soil and the lowest for the silty clay soil.

Total seasonal leaching was the lowest for subsurface drip tape (SUBTAPE), for which water and fertilizers are effectively supplied to the rooting system of the processing tomatoes. Total seasonal leaching was the highest for the surface tape system (SURTAPE), when compared to the other micro-irrigation methods, mostly because of the relatively shallow root depth of strawberries in comparison with furrow depth. We conclude that leaching potential increases as the differences between the extent of the wetted soil volume and rooting zone increases. As expected nitrate distributions for the micro-sprinkler (SPR) system were highly dependent on the non-uniform water application pattern, as most of the irrigation occurred in a small area within 1 m distance from the micro-sprinkler.

We conclude that fertigation for a short time at the end of the irrigation cycle (strategy E) generally reduces the potential of nitrate leaching in micro-irrigation systems, with the exception of surface drip and tape systems in clayey soils. Moreover, we also found that fertigation strategy is not so important for SUBTAPE systems, except that the B strategy may be favorable as it tends to retain nitrate above the drip tape by capillary action. The leached zone for the surface tape (SURTAPE) was very small compared to the other scenarios mainly because of the short irrigation time after fertigation. Long fertigation times resulted in relatively uniform nitrate distributions in the wetted regions for all but one irrigation system. For all surface-applied micro-irrigation systems on finer-textured soils, lateral spreading of water and nitrates is enhanced by surface water ponding, causing the water to spread across the surface with subsequent infiltration downwards and horizontal spreading of soil nitrate near the soil surface.

Acknowledgements

We acknowledge funding by the California FREP, Fertilizer Research and Education Program, and stimulating discussions with Dr. Keith Bristow of CSIRO Land and Water in Townsville, Australia, that initiated this research.

References

Alsinan, H.S., 1998. Uniformity of fertilizer application under micro-irrigation. M.S. thesis, Department of Land, Air and Water Resources, UC Davis.

Abbasi, F., Šimůnek, J., Feyen, J., van Genuchten, M.Th., Shouse, P.J., 2003a. Simultaneous inverse estimation of soil hydraulic and solute transport parameters from transient field experiments: homogeneous soil. Trans. ASAE 46 (4), 1085–1095.

Abbasi, F., Jacques, D., Šimůnek, J., Feyen, J., van Genuchten, M.Th., 2003b. Inverse estimation of the soil hydraulic and solute transport parameters from transient field experiments: heterogeneous soil. Trans. ASAE 46 (4), 1097–1111.

Assouline, S., 2002. The effects of microdrip and conventional drip irrigation on water distribution and uptake. Soil Sci. Soc. Am. J. 66, 1630–1636.

Bar-Yosef, B., 1999. Advances in fertigation. Adv. Agron. 65, 1–75.

Carsel, R.F., Parish, R.S., 1988. Developing joint probability distributions of soil water retention characteristics. Water Resour. Res. 24, 755–769.

Celia, M.A., Bouloutas, E.T., Zarba, R.L., 1990. A general mass-conservative numerical solution for the unsaturated flow equation. Water Resour. Res 26, 1483–1496.

Clothier, B.E., Sauer, T.J., 1988. Nitrogen transport during drip fertigation with urea. Soil Sci. Soc. Am. J. 52, 345–349.

Cote, C.M., Bristow, K.L., Charlesworth, P.B., Cook, F.J., Thorburn, P.J., 2003. Analysis of soil wetting and solute transport in subsurface trickle irrigation. Irrig. Sci. 22, 143–156.

Feddes, R.A., Kowalik, P.J., Zaradny, H., 1978. Simulation of field water use and crop yield. Simulation Monographs. Pudoc, Wageningen.

Goldberg, S.D., Gornat, B., Bar, Y., 1971. The distribution of roots, water and minerals as a result of trickle irrigation. J. Am. Soc. Hort. Sci. 96 (5), 645–648.

Hanson, B.R., Hopmans, J.W., Šimůnek, J., Gärdenäs, A., 2004. Crop nitrate availability and nitrate leaching under micro-irrigation for different fertigation strategies. FREP Progress Report, May 2004. University of California, Dept. LAWR, Davis, CA 95616.

Hanson, B.R. Unpublished data of nitrate distributions about drip lines.

Hopmans, J.W., Bristow, K.L., 2002. Current capabilities and future needs of root water and nutrient uptake modeling. Adv. Agron. 77, 104–175.

Lazarovitch, N., Šimůnek, J., Shani, U., 2005. System-dependent boundary condition for water flow from subsurface source. Soil Sci. Soc. Am. J. 69 (1), 46–50.

Li, J., Zhang, J., Rao, M., 2004. Wetting patterns and nitrogen distributions as affected by fertigation strategies from a surface point source. Agricult. Water Manag. 67, 89–104.

Mailhol, J.C., Ruelle, P., Nemeth, I., 2001. Impact of fertilization practices on nitrogen leaching under irrigation. Irrig. Sci. 20, 139–147.

Michelakis, N., Vougioucalou, E., Clapaki, G., 1993. Water use, wetted soil volume, root distribution and yield of avocado under drip irrigation. Agricult. Water Manag. 24, 119–131.

Mmoloawa, K., Or, D., 2000. Root zone solute dynamics under drip irrigation: a review. Plant Soil 222, 163–190.

Schaap, M.G., Leij, F.L., 1998. Database-related accuracy and uncertainty of pedotransfer functions. Soil Sci. 10, 765–779.

Schwankl, L.J., Prichard, T., 2001. Chemigation in Tree and Vine Micro-irrigation Systems. ANR Publication 21599, University of California, Oakland, CA 94608-1239.

Šimůnek, J., Šejna, M., van Genuchten, M.Th., 1999. The Hydrus2D Software Package for Simulating Two-Dimensional Movement of Water, Heat, and Multiple Solutes in Variable Saturated Media. Version 2.0. IGWMC-TPS-53, International Ground Water Modeling Center, Colorado School of Mines, Golden, Colorado, pp. 1–251.

Skaggs, T.H., Trout, T.J., Šimůnek, J., Shouse, P.J., 2004. Comparison of Hydrus2D simulations of drip irrigation with experimental observations. J. Irrig. Drainage Eng. 130 (4), 304–310.

Somma, F., Clausnitzer, V., Hopmans, J.W., 1998. Modeling of transient three-dimensional soil water and solute transport with root growth and water and nutrient uptake. Plant Soil 202, 281–293.

Stevens, R.M., Douglas, T., 1994. Distribution of grapevine roots and salt underdrip and full-ground cover microjet irrigation systems. Irrig. Sci. 15, 147–152.

Van Dam, J.C., Huygen, J., Wesseling, J.G., Feddes, R.A., Kabat, P., van Walsum, R.E.V., Groenendijk, P., van Diepen, C.A., 1997. Theory of SWAP Version 2.0. SC-DLO, Wageningen Agricultural University, Report 71, Department of Water Resources, The Netherlands.

van Genuchten, M.Th., 1980. A closed-form equation for predicting the hydraulic conductivity of unsaturated soils. Soil Sci. Soc. Am. J. 44, 892–898.

Vrugt, J.A., Hopmans, J.W., Šimůnek, J., 2001. Calibration of a two dimensional root water uptake model. Soil Sci. Soc. Am. J. 65 (4), 1027–1037.

Wooding, R.A., 1968. Steady infiltration from large shallow circular pond. Water Resour. Res. 4, 1259–1273.